

FRACTURE TOUGHNESS OF CERAMICS BY THE SURFACE CRACK IN FLEXURE (SCF) METHOD

G. D. Quinn¹, R. J. Gettings¹, and J. J. Kübler²

¹Ceramics Division
National Institute of Standards and Technology
Gaithersburg, MD 20899 USA

²Swiss Federal Laboratories for
Materials Testing and Research
Dübendorf, Switzerland

INTRODUCTION

The surface crack in flexure (SCF) method, also known as the controlled surface flaw method, follows conventional practice to measure fracture toughness: a specimen is precracked, the specimen is fractured, the precrack size is measured, and the toughness is computed from a well-defined stress intensity formula. A Knoop indenter is used to make the precrack in a common bend bar (Figure 1). In brittle materials, the Knoop indenter not only forms the impression, but also a semicircular or semielliptical crack under the surface with a diameter approximately equal to the length of the Knoop hardness impression. A key virtue of the method is that the precrack is very small, on the order of size of the real flaws in a ceramic and the precrack size can be controlled by the use of different indentation loads. Fractographic techniques are needed to see and measure the precrack. The SCF method has been used for over 20 years and has gained widespread acceptance for producing accurate test results. In the instances where R-curve behavior is present, the method gives a fracture toughness for the small crack portion of the R-curve.

This paper presents refinements to the SCF method, results on new materials, results from an international round robin, and statistics which demonstrate the excellent precision of the method. The SCF method is one of three that has been incorporated into an ASTM draft standard test method.

The SCF procedure was developed in the early 1970's as an alternative to classic fracture mechanics tests using large saw-cut precracks. Hardness machines with Knoop or Vickers diamonds can make an indentation and a subsurface crack in flexure specimens. For his fracture studies Kenny¹ put a row of Knoop indentations across the face of a cemented tungsten carbide specimen to create a single-edge cracked beam specimen. Kinsman et al.² carried the method further by applying only one Vickers indentation.

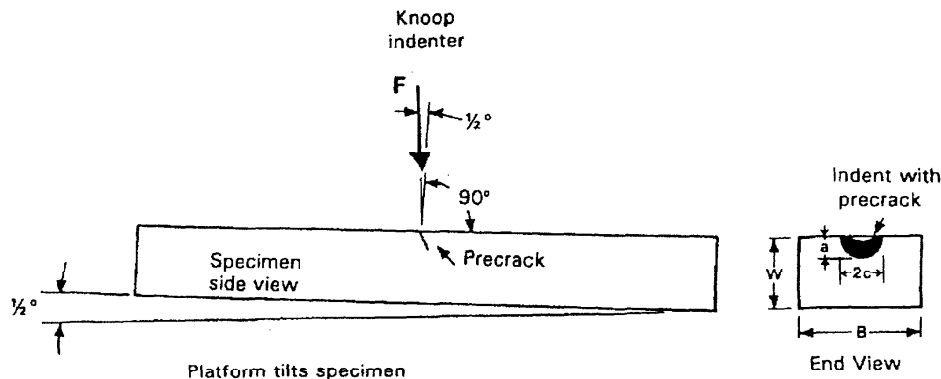


Figure 1. A Knoop indenter is used to form a semielliptical precrack in a flexure specimen. The precrack size is exaggerated in the cross section view of the specimen shown on the right. The specimen tilt (also exaggerated) is meant to aid precrack detection during fractographic analysis.

Petrovic et al.²⁵ Then made the critical observation that residual stresses under the indentation influenced the fracture toughness and demonstrated that annealing or polishing were effective means to eliminate the residual stresses. They precracked with a Knoop indenter since the crack system is much simpler. Only one primary median crack is formed and lateral cracks are less of an interference, unlike the case with Vickers indentation precracks. Knoop precracks are larger than those produced by Vickers indenters at the same load.^{6,7}

Fracture toughness (K_{Ic}) is calculated from the formula for a semicircular or semielliptical surface crack in tension or flexure:

$$K_{Ic} = Y \sigma \sqrt{a} \quad (1)$$

where: Y is the stress intensity shape factor
 σ is the flexure strength of the specimen (MPa)
 a is the crack depth (m)

This simple formula illustrates that only two things need be measured: the stress at fracture and the crack size. Y is dimensionless and is a function of the crack size and shape. The fracture stress can be measured very accurately and precisely using one of several practical, yet technically rigorous flexure strength standard test methods (e.g. ASTM C 1161⁸ or ENV 843⁹). The crack size must be measured by fractographic analysis and some care and skill is needed to find and measure the precrack.

Many investigators have utilized the Knoop SCF method for fracture toughness evaluation or for crack growth studies as chronicled in Reference 10. The method has been used successfully and given credible results on: hot-pressed, sintered, hiped, and reaction-bonded silicon nitrides; hot-pressed, sintered, and reaction-bonded silicon carbides; tungsten carbide; titanium carbide; magnesium aluminate spinel; glasses; glass ceramics;

and sintered and hot-pressed aluminas. In the instances where different investigators or laboratories have tried the same material, precrack size measurements have often been very consistent (e.g., References 3, 11 and 12).

The method is very similar to the new ASTM standard practice for metals: E 740-88, "Fracture Testing with Surface-Crack Tension (SCT) Specimens"¹³ in which semielliptical surface cracks are introduced by machining followed by fatigue precracking. ASTM standard E 740 states: "A number of different types of fracture specimens have been developed to date. Of these, the SCT specimen is one of the most representative of structures with defects that actually occur in service." It is also noted that the user must be cautious if stable crack extension occurs during the test, and the convention is to compute a nominal fracture toughness based on original crack dimensions and maximum load. These observations are germane to ceramic fracture as well. To maintain consistency with fracture mechanics terminology conventions, we will hereafter continue to refer to the method described below as the surface crack in flexure (SCF) method.

The SCF method will not work on all ceramic materials. The following criteria must be met:

1. The material must be hard and brittle.
2. It must be possible to detect the precracks.
3. The precrack size should be larger than the natural flaws in the material.

Difficulties arise if the material is coarse-grained, porous, or too tough, and with soft or porous materials, cracks will not form under the indentation. Materials with too high a fracture toughness will form very small precracks which are removed when the indentation is removed in the polishing step. In some materials the precracks may not be flat, but may be irregular since the precracks form along density or microstructural variations. The precrack size should be some multiple of the grain size in order to assure that the measured toughness is a polycrystalline fracture toughness (rather than a single crystal fracture toughness).

In general, the SCF method is regarded as producing credible results for fracture toughness which often agree with data produced by other rigorously-conducted fracture mechanics procedures. The method apparently was held in high regard by the Japan Fine Ceramics Association and was the last candidate method to be removed in the "weeding-out" process that led to creation of JIS R 1607, Fracture Toughness of High Performance Ceramics.¹⁴ The difficulty in detecting the precracks and the fact the method did not work for zirconia were the primary reasons.¹⁵ As will be shown below, however, we have devised a modification to the SCF method such that good results can be obtained for zirconia. Evans¹⁶ summarized the state of indentation microflaw testing: "Many of the indentation methods are only approximate and do not provide the quality of fracture resistance data needed to rigorously relate toughness to microstructure. The surface flaw methods, introduced first by Petrovic and Jacobson, seem to be the most precise, provided that residual stresses are eliminated by polishing out the plastic zone."

PROCEDURE

This paper summarizes results from three related studies.^{10,17,18} Tracy and Quinn¹⁷ applied SCF the method to 10 ceramics and used a variety of precracking loads. More recently Gettings and Quinn¹⁸ refined the experimental procedures particularly the methodology of precrack detection and evaluated 15 new materials. A constant 49N (5 kgf) load was used for precracking. We also include a summary of results from a twenty laboratory, Versailles Advanced Materials and Standards (VAMAS) international round

Table 1 Materials tested. Abbreviations are: (ρ) density, (E) elastic modulus, (ν) Poisson's ratio, (HP) hot pressed, (HIP) hot-isostatic pressed, (RB) reaction-bonded, (GPS) gas-pressure sintered. (*) The SNW 1000 specimens had a lower density than normal for this material.

Material	Code and/or Source	Processing	ρ (Mg/m ³)	E (GPa)	ν
Si ₃ N ₄	NC 132, Norton	HP	3.23	320	0.27
Si ₃ N ₄	NCX 34, Norton	HP	3.37	310	0.27
Si ₃ N ₄	147A (MgO), Ceradyne	HP	3.17	291	0.27
Si ₃ N ₄	NBD 200, Cerbec	HIP	3.16	320	0.26
Si ₃ N ₄	NT 154, Norton	HIP	3.23	320	0.27
Si ₃ N ₄	EKasin, ESK	HIP	3.18	315	0.27
Si ₃ N ₄	NCX 5102, Norton	HIP	3.23	--	--
Si ₃ N ₄	EC 141, NTK	GPS	3.22	310	0.26
Si ₃ N ₄	SNW-1000*, Wesgo	sintered	3.06	248	0.27
Si ₃ N ₄	KBI	RB	2.58	200	0.22
Si ₃ N ₄	NC 350, Norton	RB	2.53	180	0.22
Syalon	201, Lucas	sintered	3.24	321	0.29
SiC	NC 203, Norton	HP	3.36	460	0.17
SiC, Si	NC 435, Norton	siliconized	2.99	350	0.18
α -SiC	SA, Carborundum	sintered	3.12	410	0.15
Al ₂ O ₃	Refraceram, Asahi	sintered	3.92	--	--
Al ₂ O ₃	AD 94, Coors	sintered	3.51	291	0.23
Al ₂ O ₃	AD 999, Coors	sintered	3.96	386	0.21
Al ₂ O ₃ /SiC	ARCO	HP	3.70	401	0.24
Al ₂ O ₃ /SiC	ARCO	HP	3.70	401	0.24
B ₄ C	Ceradyne	HP	2.48	~455	--
TiB ₂	Ceradyne	HP	4.51	545	0.11
TiB ₂	LANL	sintered	4.55	557	0.13
TiB ₂	3120, Osram/Sylvania	GPS	4.64	542	0.12
TiB ₂	3122, Osram/sylvania	GPS	4.67	581	0.12
Y-TZP	EMPA	sintered, HIP	6.03	211	0.31
Glass	BK 7, Schott	melt	2.51	82	0.21

robin project which applied the method to two silicon nitrides and one zirconia.¹⁰ All materials evaluated in these programs are listed in Table 1*. The material's source and code numbers appear along with available data such as processing method, density, elastic modulus, and Poisson's ratio. The data was taken from commercial manufacturer's data or published dynamic (ultrasound or resonance) data. The test materials were procured in the form of billets or plates from which standard 3 x 4 x 50 mm flexure bars typically were machined. The alumina-silicon carbide specimens were smaller: 1.5 x 2 x 25 mm.

A Knoop indenter was used to precrack the specimens. Tracy and Quinn¹⁷ used loads of 29.4-279 N (3-28.5 kgf) depending upon the material in order to create larger or smaller precracks as needed. We subsequently have adopted 49 N (5 kgf) as our standard indentation load. Loads of 24.5, 49, and 147 N (2.5, 5, 15 kgf) were used for the three materials in the round robin. In the latter two projects, the specimen was tilted 1/2° off perpendicular to the diamond indenter axis as illustrated in Figure 1. The resultant precrack is at a slight angle to the fracture surface and introduces a negligible Mode II

*Certain commercial materials or equipment are identified in this report to specify adequately the experimental procedure. Such identification does not imply endorsement by the National Institute of Standards and Technology or the Swiss Federal Laboratories for Materials Testing and Research, nor does it imply that these materials or equipment are necessarily the best for the purpose.

component of loading during subsequent testing.¹⁰ The tilt makes precrack detection much easier during subsequent fracture surface examination. The specimen tilt was used in our more recent work¹⁸ and in the VAMAS round robin.

After indentation, it is necessary to remove the indentation and the damage zone underneath in order to eliminate the residual stresses associated with the indentation.³⁻⁵ Although polishing and/or annealing can be done, polishing is preferred since annealing carries the risk of crack blunting or healing. The amount to polish away has been empirically determined to be about 3-4X, where X is the depth of the Knoop impression.^{3-6,17} In our earlier studies, we removed 4.0X, but in several instances when there were enough specimens available, differing amounts of material (from 0 - 4.0X) were removed to confirm that 3.0X is adequate to eliminate the residual stresses. In our recent studies and the round robin, up to 4.5X was removed in order to make a more shallow precrack such that the maximum stress intensity would be located at the deepest point of the precrack. The material is removed by dry hand polishing with silicon carbide papers (180-600 grit) using common mechanical rotary polishers. A hand micrometer with a resolution of 0.002 mm was used to monitor the amount removed. Grinding with a 400 grit diamond wheel was necessary for the boron carbide and titanium diborides. The round robin participants used a variety of material removal processes.

Flexure strength was conducted using a standard 20 x 40 mm fully-articulating four-point fixture at a crosshead speed of 0.5 mm/min in accordance with ASTM C 1161 and ENV 843-1. The alumina composite specimens were tested on a 10 x 20 mm semi-articulating flexure fixture. These standard procedures measure the fracture stress with an accuracy and precision within 1-2%.

Precrack size was then measured on the fracture surface. The precrack tilt cited above helps the precrack stand out on the fracture surface. Optical and scanning electron microscopy were used, but the latter was usually more useful especially when stereo pairs of photos were taken. Our best precrack measurement procedure was as follows. Specimens were examined with a stereo optical microscope and the best fracture surface was selected for electron microscopy. The specimen was mounted in the SEM and a low magnification photo taken. Hackle lines leading from the origin readily showed the precrack region. Two higher magnification photos, typically at 200-300x, one tilted 15° relative to the other (a stereo pair) were taken of the precrack and then viewed in a stereo viewer. Stereo viewing usually made the precracks much easier to discern. A variety of features including color, contrast, brightness, ridge or rim lines, halos, and microhackle line redirection helped to delineate the precracks. If there was any doubt, the second fracture half of the specimen was examined. Additional details on precrack detection are presented elsewhere.^{10,19}

The stress intensity shape factors, Y, for semicircular and semielliptical surface cracks in bending are from the empirical equation developed by Newman and Raju.²⁰ Y depends upon the ratio of a to c, and their sizes relative to the specimen cross section. Y takes into account the bending stress fields. The Y factor is not constant and varies along the precrack boundary. *It is important to take this into account and to use the maximum value of Y* which will either be at the deepest point of the precrack, or where the precrack intersects the surface. Fracture from the former location is preferred and can be promoted by polishing sufficient material off the specimen so as to make the precrack a shallow ellipse. In some materials (that left clear fracture markings) it was possible to confirm that fracture did initiate from the point of the periphery where Y was maximized. It is also important to calculate the Y maximum for each and every precrack, rather than use a single average value.¹⁰ The Newman-Raju formulas for Y are widely accepted and it is estimated that they are accurate to within a few percent. The new ASTM standard, E 740, uses them for fracture toughness of metallic materials.

Zirconia is very resistant to precracking with the Knoop indenter. Only shallow

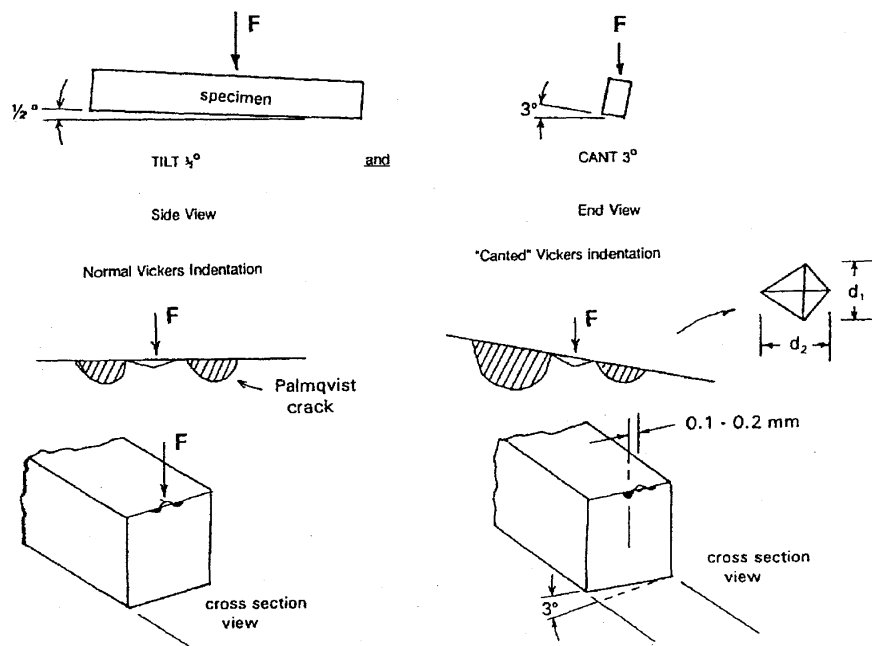


Figure 2 A tilted and canted specimen was necessary for precracking the zirconia in the international round robin.

Palmqvist cracks form on the side of the indentation at loads as high as 490 N (50 kgf). An innovative, new indenting procedure shown in Figure 2 with a tilted and canted Vickers indenter was used for the round robin. The specimen was canted on its side so that one of the Palmqvist cracks would be larger than the other. The specimen was also tilted in order to enhance precrack detectability. The indentation load was 145 N (15 kgf). 2.5X was removed from the surface after indentation in order to remove the residual stresses and leave a slightly skewed semielliptical surface crack.

RESULTS

The results from these studies are summarized in Tables 2-4. The first two columns identify the material and the next four columns describe fractographic features pertaining to the precrack as it appears on the fracture surface. "Halo" refers to a ring of different brightness around a precrack, either due to stable crack extension or crack realignment onto the primary fracture plane. Halos were obvious in the AD999 alumina and the NC132 silicon nitride. "Brightness change" refers to a difference in brightness or contrast between the precrack and the final fracture region. "Hackle lines" refers to hackle that begins, ends, or changes direction at the precrack boundary. "Overall fractographic amenability" gives a subjective ranking of the level of difficulty in fractographic analysis taking into account these and other factors. The seventh column gives the average crack size, where a is crack depth, and $2c$ is the crack width. The next column shows the ratio of successful trials per total number of specimens tested. Unsuccessful trials were those where the precracks were indistinct, oddly shaped, or incomplete, or the specimen did not break from the precrack. The last column gives the mean fracture toughness with one standard deviation uncertainty. Table 3 lists data by Tracy and Quinn¹⁷ using the same format as Table 2. In the

Table 2 Results for ceramics with a precrack from a 49 N (5 kgf) Knoop indentation.

Material	Code or source	Halo	Bright-ness change	Hackle lines	Fractographic amenity	crack size a, 2c (μm)	acpt / tested	$K_{Ic} \pm 1\sigma$ (MPa√m)
Si ₃ N ₄	NCX34	none	slight	slight	difficult	70, 184	4/5	6.35 ± .10
Si ₃ N ₄	NBD200	none	slight	clear	moderate	77, 230	5/5	5.41 ± .24
Si ₃ N ₄	NT154	none	slight	moderate	moderate	80, 206	5/5	5.80 ± .23
Si ₃ N ₄	NCX5102	none	none	moderate	difficult	59, 150	3/5	5.36 ± .62
Si ₃ N ₄	EC141	none	slight	slight	difficult	82, 219	4/5	5.22 ± .18
Si ₃ N ₄	KBI	none	none	none	not possible	--	0/5	--
Si ₃ N ₄	NC350	none	moderate	clear	easy	147, 383	4/5	1.65 ± .09
Syalon	201	none	slight	clear	moderate	100, 286	4/5	4.41 ± .12
SiC	NC203	slight	slight	moderate	moderate	133, 252	3/5	4.37 ± .38
SiC, Si	NC435	none	slight	moderate	moderate	140, 340	4/5	3.70 ± .27
Al ₂ O ₃	Referceram	none	none	slight	too difficult	--	0/6	--
Al ₂ O ₃	AD999	clear	slight	moderate	easy	119, 274	5/5	3.39 ± .09
B ₄ C	Ceradyne	none	clear	clear	easy	163, 300	5/5	3.08 ± .07
TiB ₂ 3120	Osram	none	clear	moderate	easy	121, 312	9/12	5.20 ± .41
TiB ₂ 3122	Osram	none	clear	moderate	easy	120, 304	10/12	5.36 ± .50
Glass, dry N ₂	BK7	none	clear	none	easy	229, 524	5/5	0.96 ± .09
Glass, ambient	BK7	none	clear	none	easy	219, 543	3/5	0.88 ± .09

Table 3 Results from Tracy and Quinn.¹⁷ Various indentation loads were used depending upon the material. (*) A range of loads created different sized precracks in the AD-999 alumina. (†) Precrack size varied over a wide range for the grade 147 silicon nitride.

Material	Code or source	Load P (N)	Halo	Bright-ness change	Hackle lines	Fractographic amenity	crack size a, 2c(μm)	acpt. / tested	$K_{Ic} \pm 1\sigma$ (MPa√m)
α-SiC, S	Carbor-undum	108	none	clear	clear	easy	250, 550	4/4	3.01 ± .06
SiC, HP	NC203	88	none	slight	moderate	moderate	149, 361	6/8	3.85 ± .32
Al ₂ O ₃ , S	AD999	29 - 255	clear	slight	moderate	easy	*	--	3.2 - 4.0
Al ₂ O ₃ , S	AD94	108	none	slight	slight	difficult	148, 354	5/8	3.78 ± .34
Al ₂ O ₃ /SiC	ARCO //	176	--	--	--	difficult	182, 404	2/2	6.32 ± .13
Al ₂ O ₃ /SiC	ARCO ⊥	176	--	--	--	difficult	206, 382	3/3	8.66 ± 1.54
Si ₃ N ₄ , HP	147A	108	sligh t	clear	clear	easy	†	8/10	4.70 ± .91
Si ₃ N ₄ , S	SNW1000	59	none	slight	moderate	moderate	104, 247	2/10 ⁴	4.66 ± .29
TiB ₂ HP	Ceradyne	230	--	slight	moderate	difficult	288, 689	3/3	5.52 ± .61
TiB ₂ , S	LANL	279	--	--	--	difficult	281, 561	3/3	5.14 ± .47

Table 4 Results from the VAMAS round robin. The modified Vickers precracking method was used for the zirconia.

Material	Code or source	Load P (N)	Halo	Bright-ness change	Hackle lines	Fractographic amenity	crack size a, 2c(μm)	acpt. / tested	$K_{Ic} \pm 1\sigma$ (MPa√m)
Si ₃ N ₄	NC132	24.5	clear	none	clear	easy	53, 150	107/125	4.59 ± .37
Si ₃ N ₄	ESK	49	slight	none	moderate	difficult	78, 250	105/135	4.95 ± .55
Y-TZP	EMPA	147	none	moderate	moderate	moderate	--	33/47	4.36 ± .44

instances where sufficient specimens were available, it was confirmed that 3.0X material removal after indentation was adequate to remove all residual stresses for Knoop precracks. The data for Norton NC 132 and ESK silicon nitrides and the Y-TZP zirconia in Table 4 are from the comprehensive VAMAS round robin project of 1993-1994. Twenty labs participated in this project, and the standard deviations are thus higher than what one laboratory would obtain. (The scatter that is expected for one laboratory, the within-lab repeatability, is described below.)

An important issue is how well the SCF results compare to those of other test methods. The borosilicate crown glass, Schott BK-7 (Table 2), was tested in both lab ambient and dry-nitrogen conditions. A semicircular or semielliptical precrack boundary was discerned with optical microscopy on the fracture surfaces, but it is likely that some slow crack growth caused crack extension prior to fracture in the ambient environment. The lab ambient apparent toughness is apparently lower than the dry-nitrogen toughness, but the student t statistic for two sample tests indicates the difference is not statistically significant. This probably is a consequence of the small sample sizes. In any case, the results are in excellent agreement with values of 0.86 ± 0.32 (1σ) and 0.93 ± 0.10 MPa \sqrt{m} reported by Wiederhorn and Roberts²¹ for double cantilever beam specimens tested in vacuum.

The value of 3.0 MPa \sqrt{m} that we obtained for the sintered alpha silicon carbide (Table 3) is identical to that reported by Ghosh et al.²² in their comprehensive paper on the same material. They used chevron notched specimens as well as SCF specimens. They compared their results to other data in the literature and concluded that this material has a flat R-curve and a constant toughness of 3.0 MPa \sqrt{m} .

A large data base exists for the NC-132 hot-pressed silicon nitride. Table 5 lists the available results from credible test procedures. There is a remarkable convergence of data within 4.5 to 5.0 MPa \sqrt{m} . This agreement for specimens with both large and small precracks strongly suggests that this material has a flat R-curve. Bubsey et al.²⁵ and Salem and Shannon²³ used chevron notch tests with different specimen sizes and they also concluded that the material has a flat R-curve. The mean toughness from the round robin SCF data is 4.6 MPa \sqrt{m} . This was from 107 specimens from 20 different laboratories, all of which had some measure of success in testing the material. These results are in superb agreement with the early data of Petrovic and associates³⁻⁵ from 20 years ago. The high fracture toughness from the SCF data of Gonczy and Johnson¹¹ undoubtedly is due to the crack blunting that occurred in their specimens from their air annealing treatment. The low DCB results are due to the fact that the crack ran perpendicular to the hot-pressed direction in their tests.³⁴

What results will the SCF method give for a material with a rising R-curve? Figure 3 illustrates some SCF data for a 99.9% alumina wherein the precrack size was varied over a broad range by using different indentation loads. In every instance, the residual stresses were removed by polishing 4.0 to 4.5 X after indentation. Fracture toughness results from large crack specimens are shown in the figure for comparison. The data suggest there is a small dependence of apparent toughness upon precrack size as might be expected for a material with a rising R-curve. There was some evidence of stable crack extension in the 29.4 and 49 N precracked specimens, however. The toughness results shown in Figure 3 are computed on the basis of a precrack size which does not include possible stable extension. The natural flaws in this material which limit the strength to 300-450 MPa, are primarily pores and porous zones whose size varies from 20-120 micrometers in diameter. Results from indentation strength experiments also suggest that this material may have a shallow rising R-curve.³⁰

Figure 4 shows the SCF fracture toughness for two silicon nitrides in this study as well as data from other studies using different test methods. The NC 132 data shows no trend with crack size, whereas the NCX-34 silicon nitride results do suggest an R-curve.

Table 5 Fracture toughness reported for NC-132, hot-pressed silicon nitride.

K_{Ic} MPa \sqrt{m}	Std. dev. MPa \sqrt{m}	Method	# specimens	Source
4.59	0.37	SCF	107	VAMAS Round Robin ¹⁰
4.65	0.10	SCF	-	Petrovic et al. ² **
4.64	0.25	SCF	4	Quinn and Quinn ¹² **
4.48	0.07	SCF	4	"
4.33	0.37	SCF	3	"
4.64	0.4	SCF	5	Tikare and Choi ³⁷
5.25	-	SCF	4	Gonczy and Johnson ¹¹ ***
4.5-5.0	-	NAT	6	Quinn and Quinn ¹²
4.67	0.3	SEPB	7	Tikare and Choi ³⁷
4.54	0.12	SEPB	5	Bar-on, Baratta, and Cho ³⁸ +
4.21	0.12	SEPB	10	" ++
4.5	0.4	SEPB	3	Salem et al. ^{23,24}
4.68	0.19	CN-SB	35	"
4.85	-	CN	4	"
4.64	~0.2	CN-SB	13	Bubsey, Shannon, and Munz ²⁵ *
4.72	-	CN-SB	7	"
4.71 \perp	-	CN-SB	9	"
4.83 \perp	-	CN	2	"
4.85 \perp	-	CN	2	"
4.42	0.14	CN	2	VAMAS Round Robin ¹⁰
4.58	0.10	IS	4	Kübler ³⁵
4.9	-	IS	-	Salem and Choi ²⁶
5.2	-	DT	4	Annis and Cargill ²⁷
4.9	-	DT	-	Evans and Charles ²⁶
4.1	0.21	DT	4	Govila ^{28,29}
5.8	0.74	DT	3	Quinn ³⁰
4.24	0.30	DT	-	Bansal and Duckworth ^{31,32}
4.20	0.15	FM	-	"
4.0 \perp - 5.0	-	DCB	-	Bansal and Duckworth ³³
4.0 \perp	-	DCB	30	Freiman et al. ³⁴

* Several chevron geometries and orientations.

** Several annealing conditions (air or inert atmospheres).

*** Annealed in air.

Not reported

\perp Perpendicular to the HP direction

CN Chevron Notch (Long Bar)

+

Unstable crack extension

CN-SB Chevron Notch (Short Bar)

++

Stable and semistable crack extension

DCB Double Cantilever Beam

DT

Double Torsion

SEPB Single-Edge Precracked Beam

SENB

Single-Edge Notched Beam

IS Indentation Strength (Vickers)

NAT Natural Flaws (Machining Damage) in Flexure Bars

FM Fracture Mirror Analysis, Natural Flaws

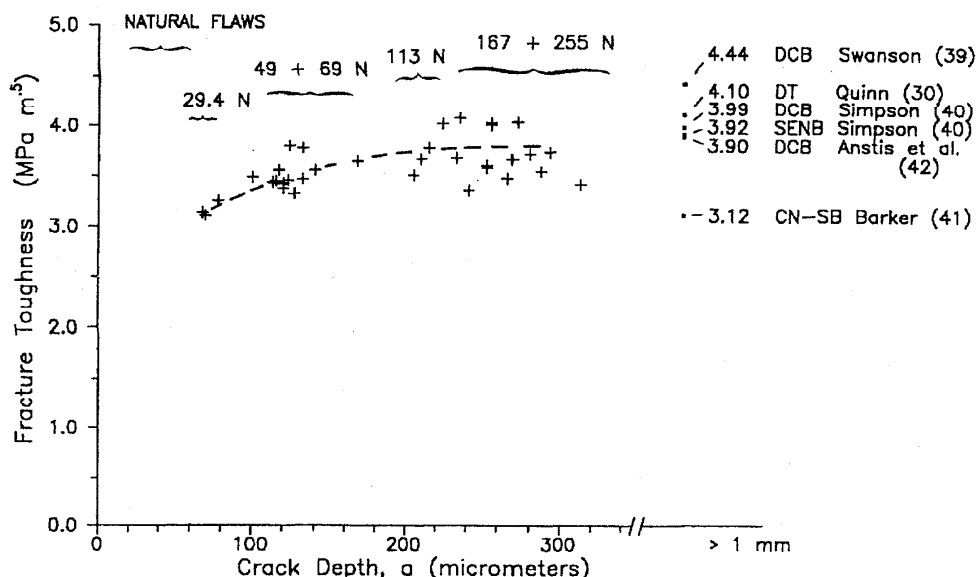


Figure 3 Apparent fracture toughness of the sintered AD-999 alumina as a function of precrack size for individual SCF specimens (+). The data on the right side (bars) are average results from large-crack fracture toughness specimens (references in parenthesis).

The dotted line for the NCX-34 is from indentation strength (IS) experiments²⁶.

The last question is whether many labs can use the SCF method successfully. The twenty laboratory VAMAS round robin investigated this.¹⁰ Some labs had used the method before while others had never tried it. All were asked to test a minimum of five specimens of the NC 132 hot-pressed silicon nitride and ten of the ESK hipped silicon nitride. Each lab received 10 specimens of each material. Each lab also received 10 zirconia specimens which were optional. The special precracking procedure shown in Figure 2 was specified for the zirconia. The grand averages and standard deviations for the three materials are listed in Table 4.

Figure 5 shows the results for the NC 132 hot pressed silicon nitride. The mean, the standard deviation, the number of specimens, and the precrack characterization method (SEM or optical microscopy) are noted for each laboratory set. The grand average toughness is shown as a dashed line. If no precrack photos were returned to the project organizers, the data set is labelled with a "?" symbol. If a lab changed their results (due to a reinterpretation of their data) this was noted by a "+". The average toughness of 107 hot-pressed silicon nitride specimens was $4.59 \text{ MPa}\sqrt{\text{m}}$ with a standard deviation of $\pm 0.37 \text{ MPa}\sqrt{\text{m}}$. Most participants had little difficulty with this material. All twenty participating labs had acceptable results and no data were rejected. Success rates (fraction of specimens tried) were usually 50-100%. Precracks were 35-55 micrometers deep and 120-160 micrometers wide. The results are in excellent agreement with the preponderance of data in the literature for NC-132 as discussed previously. We conclude that this material has a flat R-curve and a mean fracture toughness of $4.6 \text{ MPa}\sqrt{\text{m}}$ (when measured parallel to the hot-pressing direction).

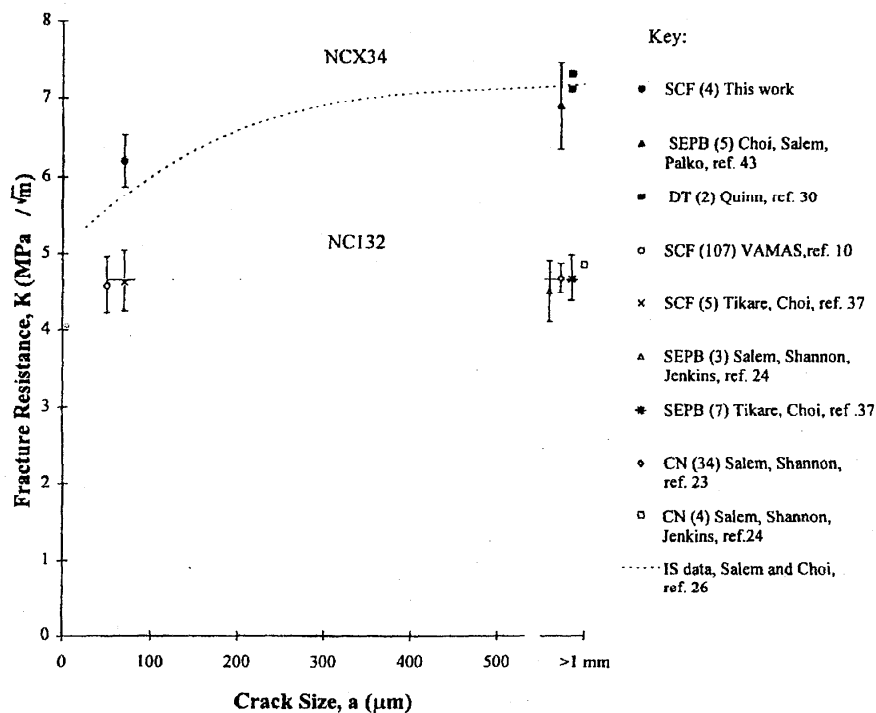


Figure 4 Fracture toughness of two hot-pressed silicon nitrides measured by five methods. The line for the NC 132 represents the average, the dashed line for the NCX-34 is an estimated R-curve on the basis of IS data. Error bars are one standard deviation, the number in parenthesis is the number of specimens tested.

The hipped silicon nitride was optional and was more challenging fractographically, but consistent results were obtained from sixteen of the eighteen labs that tried it. Precracks were 60-95 micrometers deep, and 210-270 micrometers wide. 105 specimens gave an average of 4.95 MPa/√m. Every laboratory reported at least some problem in discerning the precracks and success rates were much lower.

Testing the zirconia with the modified SCF procedure was optional, and only fourteen labs tried it. The zirconia was rather challenging, but most of the labs obtained acceptable results. Precracks were 20 to 40 micrometers deep and 45 to 80 micrometers wide. Two labs reported no success with the method at all, four labs sent results where the precracks were apparently marked incorrectly. Eight labs sent results on thirty-three specimens that were used to compute the overall fracture toughness average of 4.36 MPa/√m.

The fracture toughness results for all three materials were normally distributed.¹⁰ Additional results and analysis including controlled atmosphere testing and fifty precrack illustrations and photos are detailed in Reference 8. The VAMAS round robin results were analyzed in accordance with Standard Practice E 691⁴⁴ in order to evaluate the precision of the SCF method with the results shown in Table 6. The within-lab precision, or

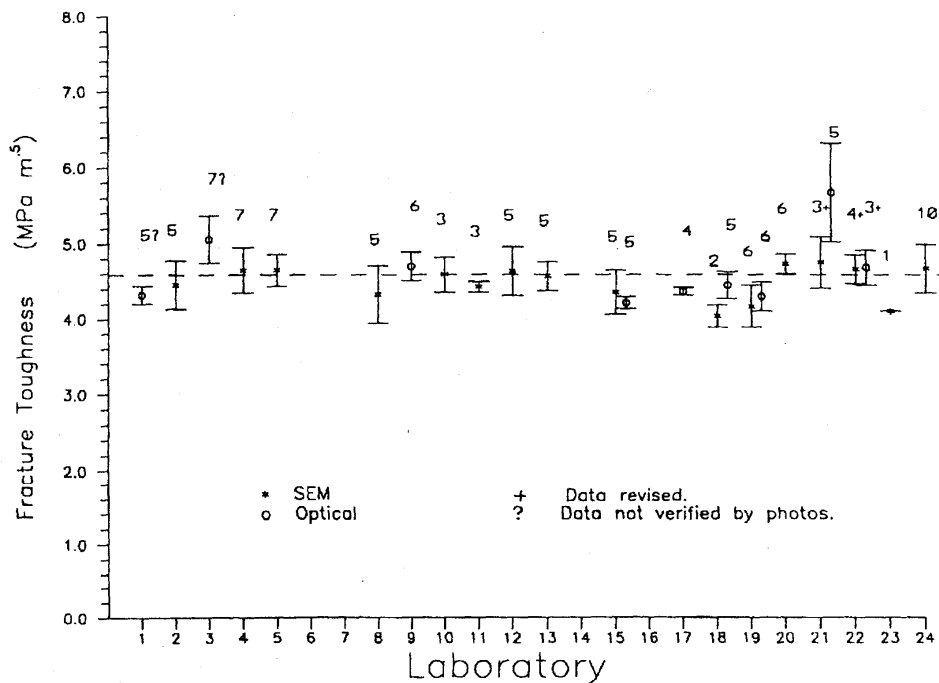


Figure 5 Results from the VAMAS round robin for the NC-132 hot-pressed silicon nitride. Each laboratory's average is shown as well as \pm one standard deviation (error bars) and the number of specimens tested.

Table 6 Precision of the SCF method based upon the VAMAS round robin results according to ASTM Standard Practice E691-92.⁴⁴ One outlier data set was removed for each material which accounts for the small difference in the average results listed in Table 4.

Material	# Labs	Total # Spec.	Average ** MPa√m	Std. Dev. ** MPa√m	Repeatability (Within-lab)		Reproducibility (Between-labs)	
					Std. Dev. MPa√m	COV % *	Std. Dev. MPa√m	COV % *
HPSN	19	102	4.56	0.32	0.24	5.4	0.31	6.8
Hipped SN	15	100	5.00	0.48	0.38	7.7	0.45	8.9
Y-PSZ	7	29	4.47	0.31	0.29	6.6	0.29	6.6

* Coefficient of variance.

** Average and standard deviation of all individual test results. Some labs tested more or less than the five specimens requested.

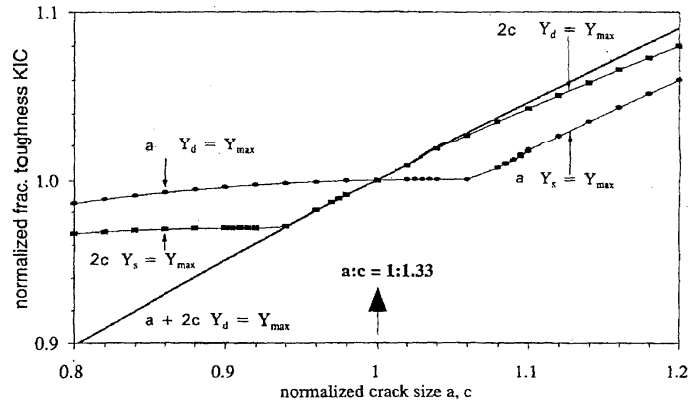


Figure 6 Uncertainty or error in fracture toughness as a function of three possible uncertainties or errors in crack size estimates: a , $2c$, or simultaneous a and $2c$. The maximum Y factor (and thus stress intensity) can either be at the surface, $Y_s = Y_{max}$; or at the deepest part of the precrack, $Y_d = Y_{max}$.

repeatability, characterizes the scatter of results obtained with the test method, in the same laboratory, by the same operator, with the same equipment, in the shortest practical period of time, using test specimens taken at random from a single quantity of material that is as nearly homogeneous as possible. The between-lab precision, or reproducibility, characterizes the variability in test results between labs.

DISCUSSION

The most difficult part of the SCF method is finding and measuring the precracks. Many of the round robin participants anguished over locating and measuring the precracks, and felt there was some subjectivity to their fractographic assessments. On the other hand, several participants reported that they had very good success with new techniques to enhance precrack detectability: tilting in the SEM, using the SEM backscattered signal, stereo SEM imaging, coating with gold in a highly directional manner, or usage of multiple photos with different magnifications.

One conclusion of the round robin was that the computed fracture toughness was *insensitive to the exact precrack boundaries marked*, because the computed fracture toughness is not sensitive to the precrack size measurement! This is partly due to the dependence of the toughness on the square root of the crack size. Thus, a 10% uncertainty (or error) in crack size is diminished to a 5% uncertainty in fracture toughness. We also discovered a fortuitous offsetting influence of Y on the errors due to crack size measurements. For example, if the crack depth is overestimated, the corresponding value of Y is underestimated. The shape of the ellipse affects the stress intensity shape factor, Y , which ranges from 1.28 to 1.99 for shallow semicircular and semielliptical surface cracks in bending. It is important that the Y factor be calculated for each and every precrack. An average Y value is not sufficient. Figure 6 illustrates how an error in the

20. J. C. Newman, Jr. and I. S. Raju, An empirical stress-intensity factor equation for the surface crack, *Eng. Fract. Mech.*, 15 [1-2] (1981) 185-192.
21. S. M. Wiederhorn and D. E. Roberts, Fracture mechanics study of skylab windows, National Bureau of Standards Report #10 892, May, 1972.
22. A. Ghosh, M. G. Jenkins, K. W. White, A. S. Kobayashi, and R. C. Bradt, Elevated-temperature fracture resistance of a sintered α -silicon carbide, *J. Am. Ceram. Soc.*, 72 [2] (1989) 242-247.
23. J. A. Salem, and J. L. Shannon, Jr., Fracture toughness of Si_3N_4 measured with short bar chevron-notched specimens, *J. Mat. Sci.*, 22 (1987) 321-324.
24. J. A. Salem, J. L. Shannon, Jr., and M. Jenkins, Some observations in fracture toughness and fatigue testing with chevron-notched specimen, pp. 9-25 in Chevron-Notch Fracture Test Experience: Metals and Non-Metals, ASTM STP 1172 eds. K. R. Brown and F. I. Baratta, ASTM, Phil., PA., 1992.
25. R. T. Bubsey, J. L. Shannon, Jr. and D. Munz, Development of plane strain fracture toughness test for ceramics using chevron notched specimens, pp. 753-771 in "Ceramics for High Performance Applications III, Reliability," Plenum, NY, 1983.
26. J. A. Salem and S. R. Choi, Toughened ceramics life prediction, pp. 220-234 in "Ceramics Technology Project Bimonthly Progress Report," Oct.-Nov. 1991, Oak Ridge National Laboratory, Oak Ridge, TN, 1991.
27. C. G. Annis and J. S. Cargill, Impact fracture of ceramics at high temperature, pp. 737-744 in "Fracture Mechanics of Ceramics, Vol. 4," eds. R. C. Bradt, D. P. H. Hasselman and F. F. Lange, Plenum, NY, 1978.
28. R. K. Govila, Material parameters for life prediction in ceramics, pp. 535-567 in "Ceramics for High Performance Applications III, Reliability," Plenum, NY, 1983.
29. R. K. Govila, Indentation precracking and double torsion methods for measuring fracture mechanics parameters in hot-pressed Si_3N_4 , *J. Am. Ceram. Soc.*, 63 [5-6] (1980) 319-326.
30. G. D. Quinn, Unpublished results.
31. G. K. Bansal and W. H. Duckworth, Effects of specimen size on ceramic strength, pp. 189-204 in "Fracture Mechanics of Ceramics, Vol. 3," eds. R. C. Bradt, D. P. H. Hasselman, and F. F. Lange, Plenum, NY, 1978.
32. G. K. Bansal and W. H. Duckworth, Fracture toughness of hot-pressed Si_3N_4 , *Am. Ceram. Soc. Bull.*, 14 (1981) 254.
33. G. K. Bansal and W. H. Duckworth, Fracture surface energy measurements by the notched beam technique, pp. 38-46 in "Fracture Mechanics Applied to Brittle Materials," ASTM STP 678, ed. S. W. Freiman, ASTM, Philadelphia, PA, 1979.
34. S. W. Freiman, A. Williams, J. J. Mecholsky, Jr., and R. W. Rice, Fracture of Si_3N_4 and SiC , pp. 824-834 in "Ceramic Microstructures 1976," eds. R. M. Fulrath and J. A. Pask, Westview Press, Boulder, Co, 1977.
35. J. J. Kübler, Unpublished research.
36. A. G. Evans and E. A. Charles, Fracture toughness determinations by indentation, *J. Am. Ceram. Soc.*, 59 [7-8] 371-372.
37. V. Tikare and S. R. Choi, Combined mode I and mode II fracture of monolithic ceramics, *J. Am. Ceram. Soc.*, 76 [9] (1993) 2265-2272.
38. I. Bar-on, F. I. Baratta, and K. Cho, Crack stability and its effect on fracture toughness of HPSN, to be publ. *J. Am. Ceram. Soc.*
39. G. D. Swanson, Fracture energies of ceramics, *J. Am. Ceram. Soc.*, 55 [1] (1972) 48-49.
40. L. A. Simpson, Discrepancy arising from measurement of grain-size dependence of fracture energy of Al_2O_3 , *J. Am. Ceram. Soc.*, 56 [11] (1973) 610-611.
41. L. M. Barker, Short rod K_{Ic} measurements on Al_2O_3 , pp. 483-494 in "Fracture Mechanics of Ceramics, Vol. 3," 1978.
42. G. R. Anstis, P. Chantikul, B. R. Lawn, D. B. Marshall, A critical evaluation of indentation techniques for measuring fracture toughness: I, Direct crack measurements, *J. Am. Ceram. Soc.*, 64 [9] (1981) 533-538.
43. S. R. Choi, J. A. Salem, and J. L. Palko, Comparison of tension to flexure to determine fatigue life prediction parameters at elevated temperatures, pp. 98-111 in "Life Prediction Methodologies and Data for Ceramic Materials," ASTM STP 1201, eds. C. Brinkman and S. Duffy, ASTM, Phil., PA, 1994.
44. E 691-92, Practice for conducting an interlaboratory study to determine the Precision of a test method, Annual Book of ASTM Standards, Vol. 14.02.